Hindawi
Journal of Nanomaterials
Volume 2022, Article ID 3491267, 14 pages
https://doi.org/10.1155/2022/3491267

Research Article

Antimicrobial Properties of *Strychnos phaeotricha* (Loganiaceae) Liana Bark Secondary Metabolites at the Interface of Nanosilver Particles and Nanoencapsulation by Chitosan Transport Vehicles

Armel Florian Tchangou Njiemou,[1] Awawou Paboudam Gbambie,[2] Simone Veronique Fannang,[1] Antoine Vayarai Manaoda,[1] Vasily Gvilava,[3] Alex Spieß,[3] Gildas Fonye Nyuyfoni,[2] Nelie Alida Mepoubong Kegne,[1] Agnes Antoinette Ntoumba,[4] Philippe Belle Ebanda Kedi,[4] Bertin Sone Enone,[1] Francis Ngolsou,[1] Jean Yves Sikapi Fouda,[1] Joel Olivier Avom Mbeng,[1] Mesode Nnange Akweh,[1] Armelle Michelle Houatchaing Kouemegne,[1] Daniel Aurelien Yana,[2] Geordamie Chimi,[5] Alex Vincent Somba,[6] Vandi Deli,[1] Emmanuel Nnanga Nga,[1] Francois Eya'ane Meva,[1] and Christoph Janiak[3]

[1]*Department of Pharmaceutical Sciences, Faculty of Medicine and Pharmaceutical Sciences, University of Douala, PO Box 2701 Douala, Cameroon*
[2]*Department of Chemistry, Faculty of Science, University of Yaounde I, PO Box 819 Yaounde, Cameroon*
[3]*Institute of Inorganic and Structural Chemistry, Heinrich-Heine-University Düsseldorf, 40204 Düsseldorf, Germany*
[4]*Department of Animal Biology and Physiology, Faculty of Science, University of Douala, PO Box 24157 Douala, Cameroon*
[5]*Department of Chemistry, Faculty of Sciences, University of Douala, PO Box 24157 Douala, Cameroon*
[6]*Department of Chemistry, Faculty of Sciences, University of Dschang, PO Box 67 Dschang, Cameroon*

Correspondence should be addressed to Francois Eya'ane Meva; mevae@daad-alumni.de

Received 11 November 2021; Revised 17 February 2022; Accepted 30 April 2022; Published 20 May 2022

Academic Editor: Lavinia Balan

Copyright © 2022 Armel Florian Tchangou Njiemou et al. This is an open access article distributed under the Creative Commons Attribution License, which permits unrestricted use, distribution, and reproduction in any medium, provided the original work is properly cited.

In this study, *Strychnos phaeotricha* liana bark extract was used as a metabolite container both on the surface of metallic nanosilver and encapsulated by a chitosan polymer. The plant extract was able to reduce Ag^+ into Ag^0 efficiently, and the encapsulation rate was determined. The synthesized nanoderivatives were characterized using ultraviolet-visible spectrophotometry (UV-Vis), Fourier transform infrared (FTIR) spectroscopy, powder X-ray diffraction (PXRD), scanning electron microscopy (SEM), and energy dispersive X-ray (EDX) spectroscopy. These methods allowed for the determination of grain size, elemental mapping, form, and the presence of secondary metabolites at the interface of the silver. Antimicrobial properties and the oral acute toxicity profile of the generated nanoderivatives were assessed. Overall, the results show plasmon resonance bands 380–550 nm in range and metabolites at the interface of a spherical nanosilver grain of 13.5 nm diameter in size. The hybrid nanosilver and encapsulated chitosan exhibited significant antimicrobial activity against *Salmonella spp*, *Echerichia coli*, and *Candida* spp. Both nanosilver grains and nanocapsules were found to be nontoxic at the tested doses and are potential models to prevent microbial resistance.

1. Introduction

Disease management in resource-limited countries relies on the exploitation of plant resources that are mainly used as extracts or essential oils. The rich flora, which is indispensable to the biological balance of ecosystems, undergoes gradual damage due to overexploitation. One way of preserving plant biodiversity is to advance the understanding and the value of plants' therapeutic effects. Metallic nanoparticles (NPs) and organic polymeric nanocapsules (NCs) are prominent routes to enhance the biomedical applications of plants by transporting secondary metabolites to target cells.

The use of silver at nanometric sizes is a longstanding practice that has attracted the attention of many researchers because of silver's many attractive properties [1]. Nanoparticles are aggregates of small molecules of nanometric size (dimensions between 1 and 100 nm) consisting of a few hundred to a few thousand atoms. The nanometric size increases the surface area of materials, giving them greater reactivity [2]. Biological methods of synthesizing silver nanoparticles in solution are ecoresponsible and inexpensive, making them appropriate for resource-limited countries' development.

Chitosan (Cs) is derived from chitin, which is a long polymeric chain of N-acetyl-β-D-glucosamine and D-glucosamine residues that has been randomly deacetylated. Indeed, chitin is the main component of the shell of crustaceans, but it can also be found in cuttlefish bones, squid feathers, insect cuticles, and mushrooms. Chitin is made up of more than 40% of acetyl groups [3]. Different methods such as emulsion cross-linking, coacervation/precipitation, and ionic gelation are used to prepare particulate chitosan systems. The choice of methods depends on factors such as the particle size, the thermal and chemical stability of the active agent, the reproducibility of released kinetic profiles, the stability of the final product, and residual toxicity associated with the final product [4–8].

Strychnos phaeotricha belongs to the Loganiaceae family, which includes 450 to 500 species classified into 30 genera. The genus Strychnos is widely distributed in the tropics, with nearly 75 species in Africa and Madagascar [9]. *Strychnos phaeotricha* is commonly known as "mpidi" in the Central African Republic, "fuankia" in Cameroon, "mbundu" in the Democratic Republic of Congo, "salie" in Gabon, and "malagueto" in Ghana [10]. The plant is a liana of about 35–50 m in length and 4–40 m in height; the stem is 2–7 cm or more in diameter; pale grey bark, lenticellate; twigs, lenticellate or not; small shaggy brown twigs, not lenticellate; and tendrils in pairs [10]. Studies have revealed the antimicrobial activity of indole alkaloids belonging to 40 species of the Loganiaceae family, including the genus Strychnos [11]. Chemical studies of root and stem barks have revealed the presence of various alkaloids including akagerine and its derivatives (akagerine lactone, O-ethylakagerine, and tetrahydroakagerine), ajmalicine, tetrahydroalstonine, dihydrocycloakagerine, and dihydrocorynantheol to have low muscle-relaxant, convulsant, and antimicrobial properties [12]. To the best of our knowledge, no studies have been carried out on the synthesis of silver nanoparticles and nanocapsules from *Strychnos phaeotricha* extract. Therefore, in this study, we present the antibacterial and antifungal activity followed by the oral acute toxicity profile of secondary metabolites from *Strychnos phaeotricha* liana bark fixed on silver nanoparticles and encapsulated in chitosan.



Figure 1: *Strychnos phaeotricha* liana.

2. Materials and Methods

2.1. Collection and Authentication of the Plant Material. Liana bark of *Strychnos phaeotricha* (Figure 1) was harvested in December 2019 at Mount Kala in Yaoundé and authenticated at the Cameroon National Herbarium under reference number 49110NHC. The plant material was dried in a shadow environment at room temperature for 3 weeks and then pulverized by crushing.

2.2. Extract Preparation. Extraction was carried out using water and methanol as the solvents. The aqueous extract was prepared by introducing 10 g of powdered liana bark into a conical flask containing 100 mL of preheated distilled water (80°C) and stirring for 5 minutes using a magnetic stirrer. After cooling to room temperature, the mixture was filtered using Whatman filter paper No. 1. To determine the extraction yield, part of the prepared extract was left overnight in an oven (60°C) until it had completely evaporated [13].

The methanolic extract was obtained by double maceration of 1000 g of powdered liana bark in 5000 mL of methanol for 72 hours at room temperature with regular shaking. The mixture was then filtered using Whatman filter paper No. 1 and concentrated using a rotary evaporator (REV 2000 series, Bioevopeak, Jinan City, China) at 90°C and 120 rpm. Residual solvent was eliminated by keeping the extract in an oven at 60°C [14]. The calculation of the extraction yield was carried out according to Equation (1).

$$\tau = \frac{m}{M} \bullet 100, \quad (1)$$

Table 1: Phytochemical composition of extracts.

Test		Observation	
		Methanolic extract (ME)	Aqueous extract (AE)
Polyphenols		+	+
Flavonoids		+	+
Alkaloids		+	+
Coumarins		+	+
Saponins		+	+
Terpenoids		+	-
Steroids		+	-
Reducing sugars		+	+
Anthraquinone	Link quinone	+	-
	Free quinone	-	-

Note. +: present; -: absent.

where τ is the extraction rate, M is the initial mass, and m is the mass of concentrated extract.

2.3. Synthesis of Silver Nanoparticles (AgNPs). To support the synthesis of silver nanoparticles, various volumes (5 mL, 10 mL, and 15 mL) of *Strychnos phaeotricha* liana bark aqueous extract were added to 50 mL of 10^{-1} M silver nitrate. To avoid the photoactivation of cationic silver, the mixtures were incubated in the dark at room temperature until a change in color appeared. Subsequently, 1 mL aliquots from each tube were taken at different lengths of incubation time (5 minutes, 1 hour, 3 hours, 24 hours, 1 week, and 2 weeks) for UV-visible spectrophotometric analysis (UViLine 9100, Secoman, Brussels, Belgium). In the optimization experiments, the silver nitrate concentrations (10^{-1} M, 10^{-2} M, and 10^{-3} M) and pH (2, 4, 6, 8, 10, and 12) using 0.1 N sulfuric acid or 0.1 N sodium hydroxide were varied [15].

2.4. Synthesis of Chitosan Nanocapsules (NCs). Chitosan nanocapsules were synthesized using both methanolic and aqueous extracts. A 10 mg/mL chitosan solution was freshly prepared by adding 50 g of chitosan powder to 5000 mL acetic acid solution (1% v/v), and the pH was adjusted to 5 using sulfuric acid [16]. Sodium tripolyphosphate (STPP) solution was prepared concomitantly by adding 2400 mg of STPP powder to 600 mL of distilled water. The synthesis of the nanocapsules was done by mixing 150 mg of each extract with 100 mL of prepared chitosan solution followed by 50 mL STPP solution added dropwise (25 drops/minute) under magnetic stirring (HPS 340, Bioevopeak, Jinan City, China). Thereafter, the suspension was sonicated for 30 minutes at 20% amplitude and centrifuged at 4000 rpm for 10 minutes to isolate the nanocapsules from the methanolic extract (NC-ME) or the aqueous extract (NC-AE), respectively. The metabolite encapsulation rate was determined by dosing polyphenol contents from the reaction mixture and supernatant. Empty chitosan nanocapsules (NC-E) were synthesized similarly without adding any extract.

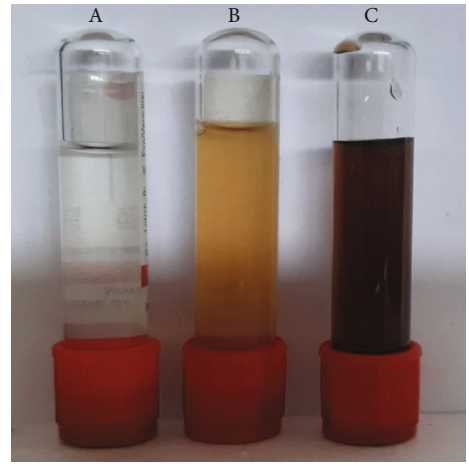


Figure 2: (A) Aqueous silver nitrate solution, (B) aqueous extract of *Strychnos phaeotricha* liana bark, and (C) silver nanoparticles formed by combining silver nitrate and the extract solution.

2.5. Total Phenolic Content and Encapsulation Efficiency Determination. The dosage of total phenols was carried out following the Folin-Ciocalteu method described by Pratiwi et al. [17]. One milliliter of each sample was added to 5 mL of a 10% Folin-Ciocalteu solution and incubated for 30 minutes. Four milliliters of sodium bicarbonate solution (0.7 M) was subsequently added to the mixture and vigorously stirred and then incubated for 2 hours at room temperature. The absorbance of the final solution was recorded at 765 nm. A range of standard using gallic acid (0.3, 0.6, 0.9, and 1.2 μg/mL) was prepared similarly for the calibration curve. The total phenolic content was determined from the regression equation of the calibration curve and expressed in milligrams, equivalent to gallic acid per gram of the weight of the extract (mg EQ/g E) [17].

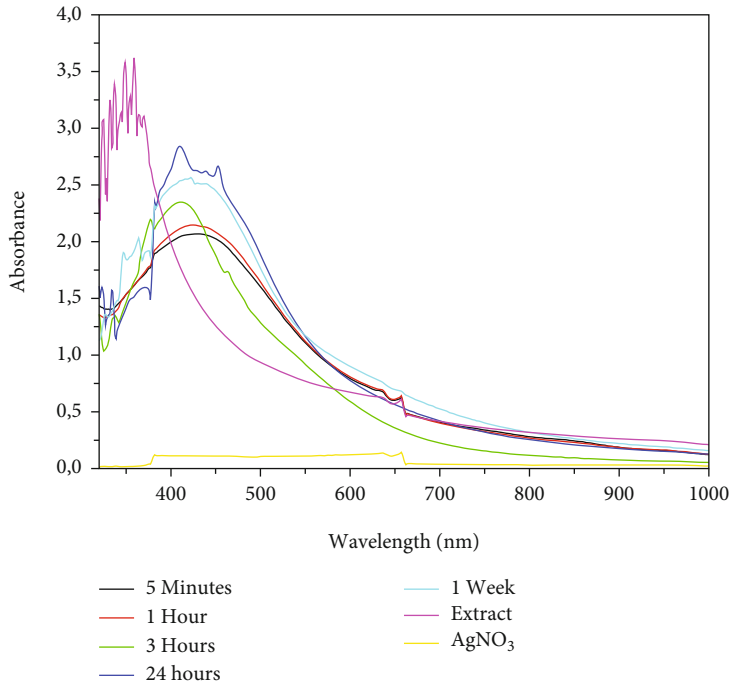
The encapsulation efficiency was calculated according to Equation (2) [16]:

$$\mathrm{EPP} = \frac{(\mathrm{TPC\ of\ the\ extract} - \mathrm{TPC\ of\ the\ NC\ supernatant})}{\mathrm{TPC\ of\ the\ extract}} \bullet 100, \quad (2)$$

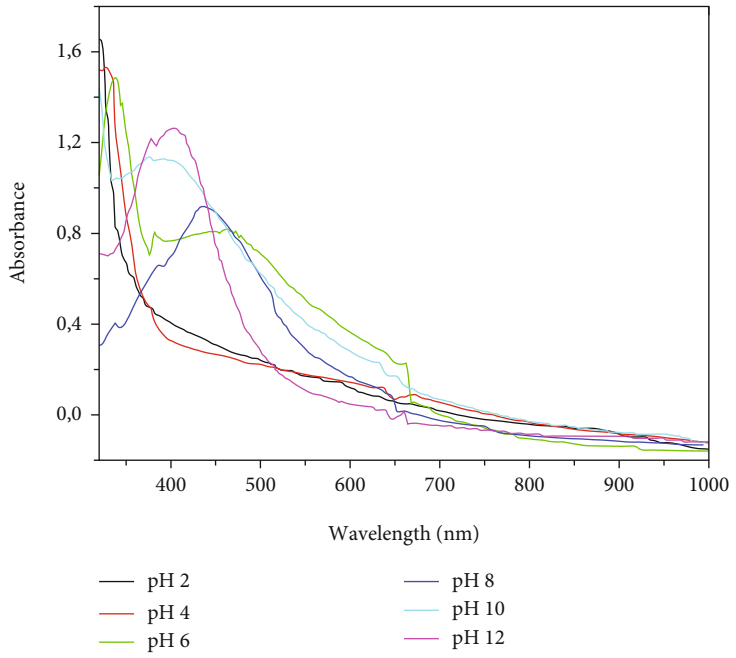
where TPC is the total phenolic content.

2.6. Phytochemical Screening. Phytochemical screening was carried out to demonstrate the presence or absence of polyphenols, flavonoids, alkaloids, reducing sugars, coumarins, triterpenes, saponins, steroids, and anthraquinones following Harbone et al. of 1999 and Evans of 2001 [18, 19].

2.7. Instrumentation. UV-Vis spectrophotometry was carried out on an UVline 9100 UV-Vis spectrophotometer (UViLine 9100, single-beam halogen light source, 1 nm resolution with a wavelength ranging from 320 to 1100 nm). Fourier transform infrared (FTIR) spectra were obtained on a Bruker FT-IR Tensor 37 spectrometer with a resolution of 2 cm^{-1} in the 4000–550 cm^{-1} region (Infrared Bruker Tensor 37, Profactor Gmbh, Vienna, Austria). All samples were measured as KBr disks. Powder X-ray diffraction

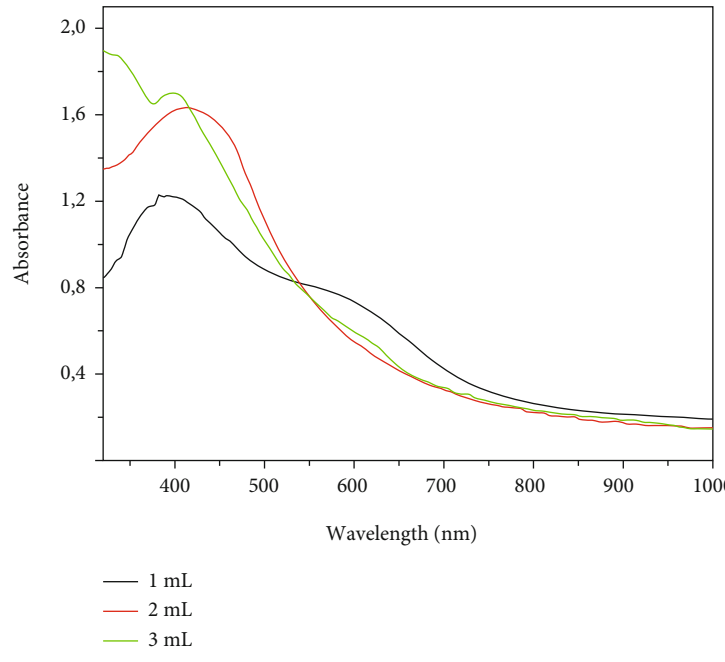


(a)

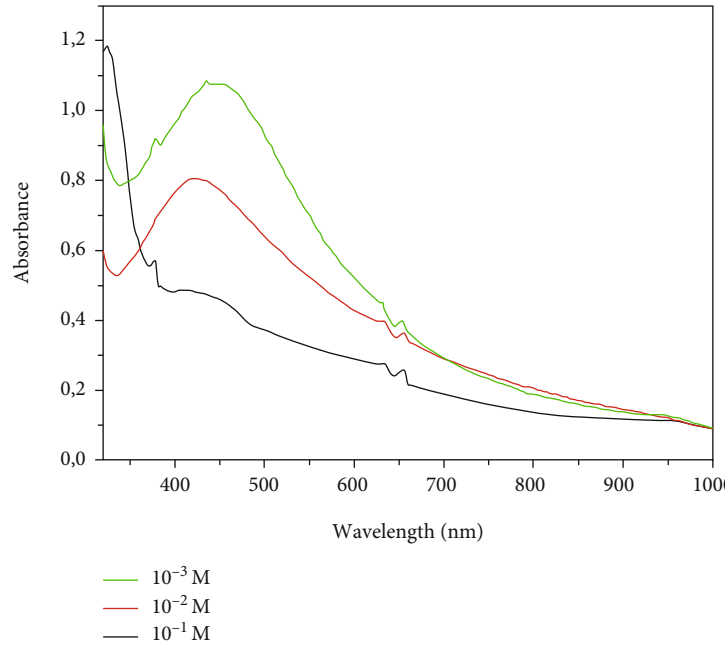


(b)

Figure 3: Continued.



(c)



(d)

Figure 3: UV-Vis absorption spectra of biosynthesized AgNPs with respect to (a) time, (b) pH, (c) extract quantity, and (d) silver nitrate concentration.

(PXRD) patterns were recorded on a Bruker D2 Phaser powder diffractometer (Bruker AXS Gmbh, Bonn, Germany) equipped with a flat silicon low-background sample holder using Cu–Kα radiation ($\lambda = 1.5418$ Å, 30 kV, 10 mA, and ambient temperature). Scanning electron microscopy (SEM) images were obtained using a Jeol JSM-6510LV QSEM advanced electron microscope equipped with a LaB6 cathode at 5–20 kV (JSM-6510-SEM, Gute Aenger, Freising, Germany). The microscope was equipped with a Bruker Xflash 410 silicon drift detector for energy-dispersive X-ray (EDX) spectroscopy. Before the scanning took place, the samples were dried at 60°C under vacuum for at least 12 hours.

2.8. Microbial Strains, Experimental Animals, and Ethics. The acute toxicity assessment of the silver nanoparticles and chitosan nanocapsules was performed on 8- to 12-week-old Wistar albino rats. The Mueller-Hinton and Dulbecco's Modified Eagle Medium obtained from Merck and HyClone, respectively, were used for the evaluation of

Table 2: Encapsulation efficiency of chitosan nanocapsules (NCs).

Extract		Total polyphenol content (mg eq of gallic acid/g of extract)	Encapsulation efficiency (%)
	AE	23.280	
NC-AE	Chitosan+AE	0.035	73.500
	Supernatant	0.009	
	ME	43.490	
NC-ME	Chitosan+ME	0.065	69.340
	Supernatant	0.020	

Note. ME: methanolic extract; EA: aqueous extract; eq: equivalent.

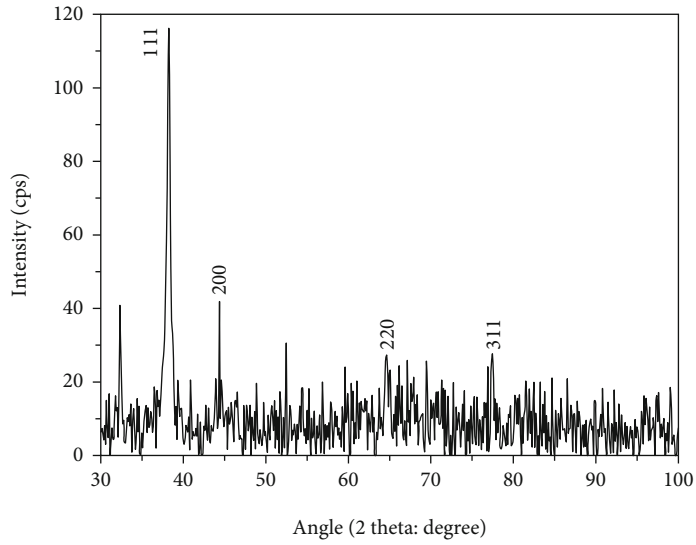


Figure 4: Powder X-ray diffractogram of the synthesized AgNPs.

antibacterial and antifungal *in vitro* activity on *Candida spp* 19060502 strains (clinical isolate resistant to fluconazole), *Escherichia coli* ATCC 25922 and *Escherichia coli* 20072302 (multiresistant clinical isolates), and the sensitive clinical isolate of *Salmonella spp* 20031204 obtained in the bacteriology laboratory of Yaoundé Hospital and University Centre (CHUY). All experimental procedures were in strict compliance with the protocol issued by the Institutional Ethical Committee of the University of Douala (protocol approval number 2185 CEI-UDo/07/2020/T).

2.9. Assessment of Oral Acute Toxicity on Wistar Rats. The oral acute toxicity test of synthesized nanoderivatives (AgNPs, NC-AE, and NC-ME) was performed according to Organization for Economic Cooperation and Development (OECD) guideline No. 425. Twelve female Wistar rats were randomly assigned to four groups of three rats each. Each of the four experimental groups was subjected to non-water fasting for 12 hours prior to AgNP, NC-AE, or NC-ME administration at a single dose of 2000 mg/kg [20]. The control group received distilled water (1 mL/100 g b.w). All substances were orally administered using an epigastric canula, and food was provided 2 hours after dosing. Animals were closely observed for first 30 min, then intermittently at 4 hours, and once at 12 hours for the next 14 days for any change in their behavioral, neurological, or autonomic profile. At the same time, their weight was recorded using a PCE-BSH® 6000 electronic scale, and the data were used to determine the growth rate according to Equation (3).

Table 3: PXRD characteristics of the synthesized AgNPs.

Peaks	Miller indices (hkl)	Position (2θ)	FWHM	Size (nm)
1	111	38.180	0.657	13.37
2	200	44.330	0.657	13.64
3	220	64.690	n.d.	–
4	311	77.340	n.d.	–
Mean				13.5

Note. n.d.: not determined as these peaks were barely above noise level.

$$\text{Growth rate} = \frac{\text{mass of rat on day x} - \text{mass of rat on day 0}}{\text{mass of rat on day 0}} \bullet 100. \quad (3)$$

At the end of the study, all rats were anesthetized using ketamine (50 mg/kg b.w) and diazepam (10 mg/kg b.w) and their blood was collected for analysis of biochemical parameters. Some vital organs including the liver, kidneys, lungs, heart, and spleen were excised, weighed, and fixed in formaldehyde buffer for histological analysis. The photographs

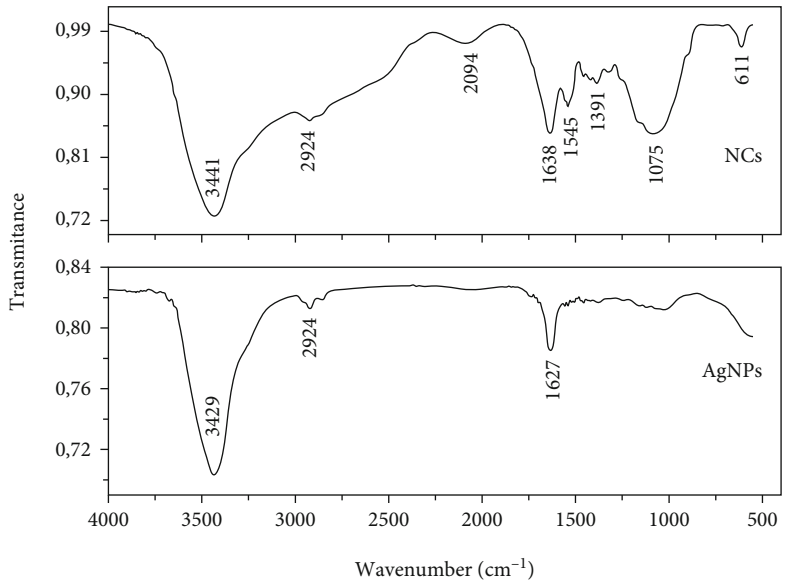


Figure 5: Infrared spectra of AgNPs and NCs.

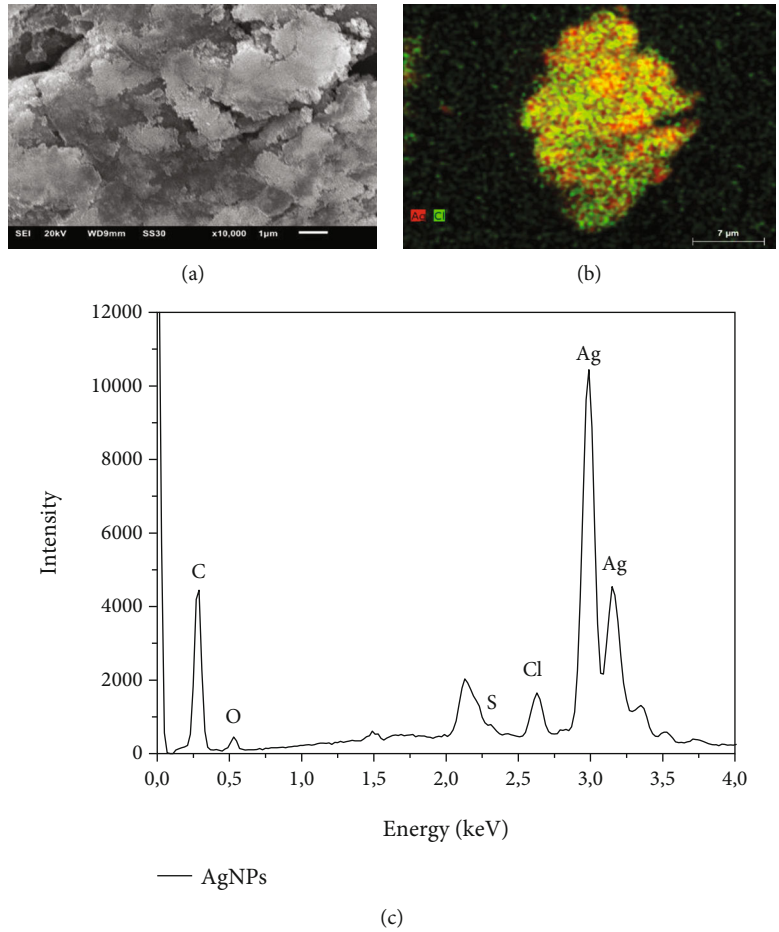


Figure 6: AgNPs' (a) SEM image, (b) EDX element mapping, and (c) EDX spectrum.

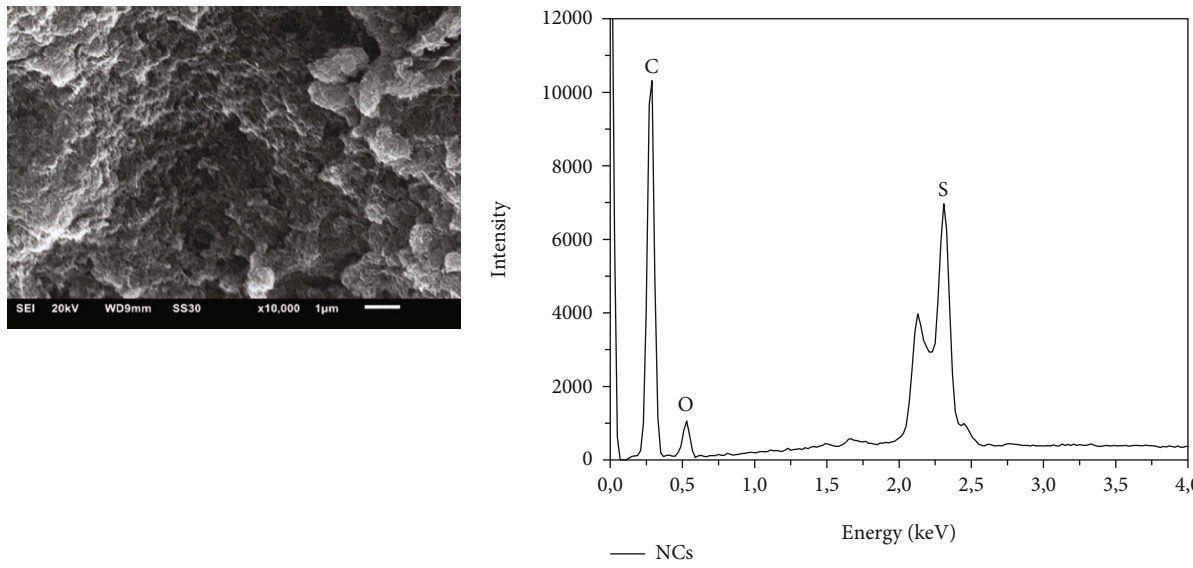


Figure 7: NCs' (a) SEM image and (b) EDX spectrum.

Table 4: EDX spectral element percentage of the synthesized AgNPs and NCs.

Element		C	Ag	O	Cl	S	Al	Si	Total
Atomic %	AgNPs	62.0	22.7	11.0	1.8	1.2	0.8	0.3	100.0
	NCs	86.5	-	9.8	-	3.7	-	-	100.0

were recorded using a Scientico STM-50® optic microscope and a Celestron® 44421 digital camera.

2.10. Evaluation of Antimicrobial Activity. To assess antimicrobial activity, bacterial strains and fungal strains were incubated with suspensions of AgNPs, NC-ME, NC-AE, and NCs at different concentrations. The method used to assess the sensitivity of bacteria and yeasts to different samples was micro dilution, as described in International Organization for Standardization (ISO) standard 20776-1 (2006) and adopted by the Antibiotic Committee of the French Society of Microbiology (CA-SFM/EUCAST 2019) [21, 22].

The method consisted of diluting the suspensions of AgNPs, NCs-AE, NCs, and NCs-ME in a liquid culture medium and inoculating the medium with the microbial strains to be tested. The minimum bactericidal concentration (MBC) was determined by subculturing 50 μL of suspension from each well in which no growth was observed in 50 μL of the corresponding culture medium. This was indeed the smallest concentration for which no growth was observed after subculturing. The MBC/MIC (MIC: minimal inhibitory concentration) ratio revealed the bacteriostatic or bactericidal nature of the active samples.

2.11. Statistical Analyses. The triplicate data reading values of inhibition zones in diameter and concentration values (MIC and MBC) were analyzed using the PRISMA software (version 8.0.1; Graphpad Software, Inc., San Diego, CA, USA). Each experimental value was expressed as mean ± ESM. The values for the treated groups and control were compared using a Student t-test, and results with p values less than 0.05 were considered significant.

3. Results and Discussion

3.1. Phytochemical Composition of Extracts. As shown in Table 1, both aqueous and methanolic extracts are rich sources of several compounds including polyphenols, flavonoids, coumarins, alkaloids, saponins, coumarins, and reducing sugars. However, terpenoids, steroids, and anthraquinones were found only in the methanolic extract. This difference might be due to the extraction method, which entailed a shorter contact time when using water than it did when using methanol. Furthermore, the greater affinity of methanol for plants' secondary metabolites could explain the high content of bioactive compound in the methanolic extracts (Table 1). The presence of flavonoids, alkaloids, and terpenes is compatible with antimicrobial activity [23]. The presence of polyphenols and terpenes is compatible with the reduction of Ag^+ to AgNPs and their stabilization [24]. Studies conducted by Bouquet and Fouret on *Strychnos phaeotricha* roots revealed only the presence of alkaloids [12]. Alkaloids are reported to possess antimicrobial activity and are able to reduce Ag^+ into Ag particles [24]. In view of these results, the extracts appear to be rather rich in metabolic diversity, making them similar to other species of the genus Strychnos.

3.2. Visual Observation and UV-Vis Spectra of Synthesized Silver Nanoparticles. AgNPs were obtained by mixing

Table 5: MIC and MBC of different samples tested against *E. coli* and *Salmonella spp* (sensitive) compared to those of ciprofloxacin.

Microbial strain	*Escherichia coli*			*Salmonella typhi*		
	MIC (mg/mL)	MBC (mg/mL)	MBC/MIC	MIC (mg/mL)	MBC (mg/mL)	MBC/MIC
ME	1.000	>1.000	/	0.125 ± 0.000	1.000 ± 0.000	4.000[$]
AE	1.000	>1.000	/	0.063 ± 0.000	0.250 ± 0.000	4.000[$]
NC-ME	0.125 ± 0.000	0.500 ± 0.000	4.000[$]	0.250 ± 0.000	1.000 ± 0.000	4.000[$]
NC-AE	0.500 ± 0.000	1.000 ± 0.000	2.000[#]	1.000 ± 0.000	>1.000	/
NC	>1.000	>1.000	/	>1.000	>1.000	/
AgNPs	0.500 ± 0.000	0.500 ± 0.000	1.000[#]	0.004 ± 0.000	0.008 ± 0.000	2.000[#]
CIPRO	0.004 ± 0.000	0.004 ± 0.000	1.000[#]	0.004 ± 0.000	0.008 ± 0.000	2.000[#]
Positive control		-			-	
Negative control		+			+	
Sterility control of the culture media		-			-	

Note. -: no growth observed; +: presence of growth; [#]bactericidal; [$]bacteriostatic. $p > 0.99$.

Table 6: MIC and MBC of promoter samples on multiresistant *E. coli.*

Microbial strain	*Escherichia coli*		
	MIC (mg/mL)	MBC (mg/mL)	MBC/MIC
NC-ME	0.5 ± 0.0	>1.0[#]	/
NC-AE	>1.0	/	/
AgNPs	0.5 ± 0.0	0.5 ± 0.0	1.0[#]
Positive control		-	
Negative control		+	
Sterility control of the culture media		-	

Note. -: no growth observed; +: presence of growth; [#]bactericidal; [$]bacteriostatic. $p > 0.99$.

Strychnos phaeotricha liana bark aqueous extract with silver nitrate solution as depicted in Figure 2. The color of the reaction mixture changed from yellowish to deep brown after 5 minutes of incubation, indicating the formation of AgNPs. Similarly, rapid reduction rate have been observed with plant leaves like carob and *Megaphrynium macrostachyum* [13, 25]. This color change is due to the reduction of Ag^+ ions into Ag^0 by secondary metabolites such as alkaloids or polyphenols. The bioreduction process can be explained by a mechanism involving the formation of quinone intermediates [24]. Such a change in coloration occurs during the collective vibration of free electrons at the surface of colloids [26].

The formation of AgNPs was confirmed by recording a surface plasmon resonance band between 380 and 550 nm on the UV-Vis spectrum. This band width indicates a relatively large size distribution of synthesized nanoparticles [27]. The AgNP formation spectrum after 24 hours of incubation showed no further increase in nanoparticle production and remained stable without any sign of coalescence (Figure 3). This stability is due to the capping of AgNPs by secondary metabolites, which prevents agglomeration [28]. The formation of AgNPs was followed by various condition changes: pH, volume of extract, and silver nitrate concentration. The formation of nanoparticles increased proportionally to the increases in pH, $AgNO_3$ concentration, and volume of extract (Figure 3). Similar observations have been made in the literature [28].

3.3. Chitosan Nanocapsule Synthesis. The formation of chitosan nanocapsules using aqueous and methanolic extracts was achieved by ionic gelation, and the encapsulation rate of secondary metabolites was estimated by dosing total phenols [17, 29]. The encapsulation rates were found to be 73.5% and 69.3% for the aqueous and methanolic extracts, respectively (Table 2). During ionic gelation, positively charged chitosan macromolecule interact electrostatically with negatively charged tripolyphosphate. Spontaneous aggregation takes place in the form of a nanosized sphere. During this aggregation process, secondary metabolites are internalized in a homogeneous manner. The obtained encapsulation percentage shows that the process does not depend on the type of extract but on other factors such as the concentration of chitosan, tripolyphosphate, extract quantity, and/or the speed of dispersion and the degree of deacetylation of chitosan as previously reported [17, 29].

3.4. Powder X-Ray Diffraction (PXRD) Analysis. PXRD analysis was performed on the synthesized silver nanoparticles to determine their crystallinity and size (Figure 4 and Table 3). The peaks obtained at the 2 theta angles of 38.18, 44.33, 64.69, and 77.34 were attributed to silver based on a

Table 7: MIC and MBC of different samples tested against *Candida spp* compared to those of ketoconazole and fluconazol.

Microbial strain	*Candida spp*		
	MIC (mg/mL)	MFC (mg/mL)	MFC/MIC
ME	>1.000	>1.000	/
AE	>1.000	>1.000	/
NC-ME	>1.000	>1.000	/
NC-AE	>1.000	>1.000	/
NC	>1.000	>1.000	/
AgNPs	0.004 ± 0.000	0.008 ± 0.000	2.000[#]
Fluconazole	>1	/	/
Ketoconazole	$0.002 * 10^{-3} \pm 0.000$	/	/
Positive control		-	
Negative control		+	
Sterility control of the culture media		-	

Note. -: no growth observed; +: presence of growth; [#]bactericidal; [$]bacteriostatic. $p > 0.99$.

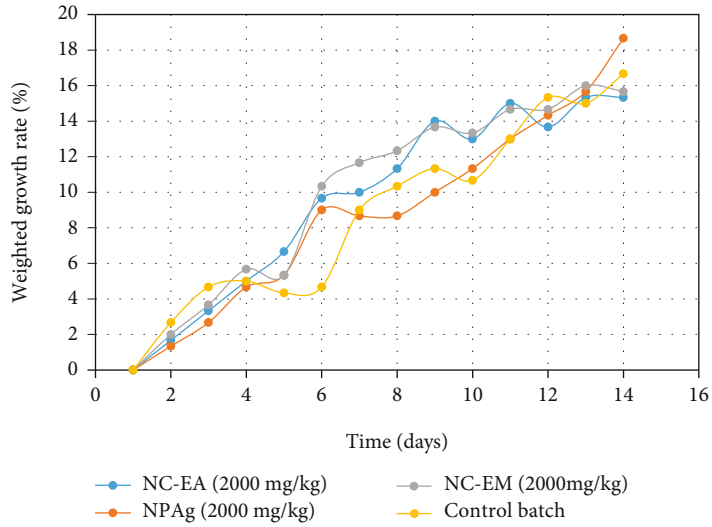


Figure 8: Evolution of rat body weight with respect to time. $p > 0.05$.

comparison with data from the COD-Inorg REV184238 database. The indexation of the peaks by the Miller indices (hkl) corresponding to the respective crystal planes of 111, 200, 220, and 311 demonstrated that the nanoparticles formed are of face-centered cubic crystal structure [13]. The theoretical average size of the synthesized nanoparticles was calculated by applying Scherrer's Equation (4). The signals at 64.69 and 77.34 were not considered in the calculation as they were barely above noise level:

$$D = \frac{0.9\lambda}{\beta \cos \theta}, \quad (4)$$

where D is the diameter of the particles, λ is the wavelength used (0.154 nm), β = FWHM/180 (FXHM: full width at half height), and θ is the diffraction angle.

An average diameter of 13.5 nm was obtained. This diameter is of the same order of magnitude as that of the nanoparticles obtained from *Persea americana* bark extract (16 ± 4 nm) [30].

3.5. Silver Nanoparticles and Nanocapsules' Surface Analysis. The functional groups present at the surface of AgNPs and NCs were determined by analyzing the FTIR spectrum, which reveals chemical bonds' elongation, vibrations, and/or deformations (Figure 5). Phenolic vibrations O-H and C-H of the alkane chains and C=O and C=C of the amide and ester functions were observed on AgNPs. Similar observations were made by Zou et al. in 2012 who hypothesized that phenolic compounds are involved in metal ion reduction and metal nanoparticle stabilization [24]. The O-H vibrations of alcohol, N-H of amines, C-H of alkane chains, C≡C of alkynes, C=C of alkenes, and C-O of ethers were observed on NCs. These functional groups characterize the chitosan nanocapsule structure as described by Servat-Medina in 2015 [16]. Indeed, the metabolites internalized in the nanocapsules are covered by chitosan whose groups are practically the only ones to appear in the spectrum.

3.6. Scanning Electron Microscopy Analysis. Scanning electron microscopy (SEM) images of both AgNPs and NCs

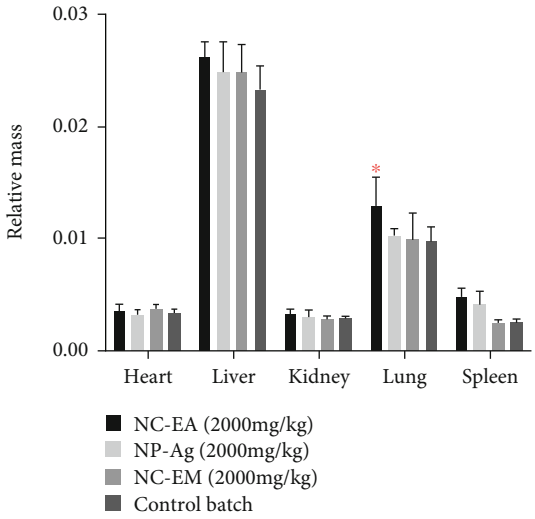


Figure 9: Weight of rat organs tested with AgNPs, NCs-ME, and NCs-AE with respect to the control. $^{*}p < 0.05$.

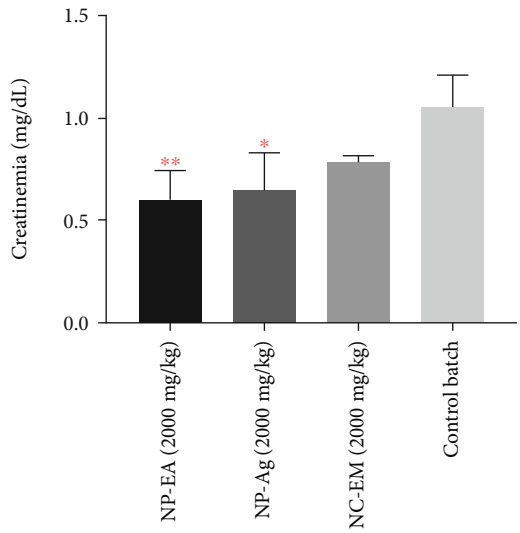


Figure 10: Creatinemia level of rats subjected to the acute toxicity test for different samples and the control. $^{*}p < 0.05$; $^{**}p < 0.01$.

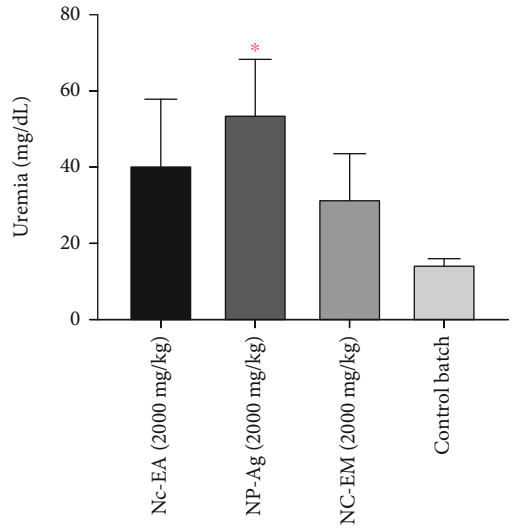


Figure 11: Uremia level of rats subjected to the acute toxicity test for different samples and the control. $^{*}p < 0.05$.

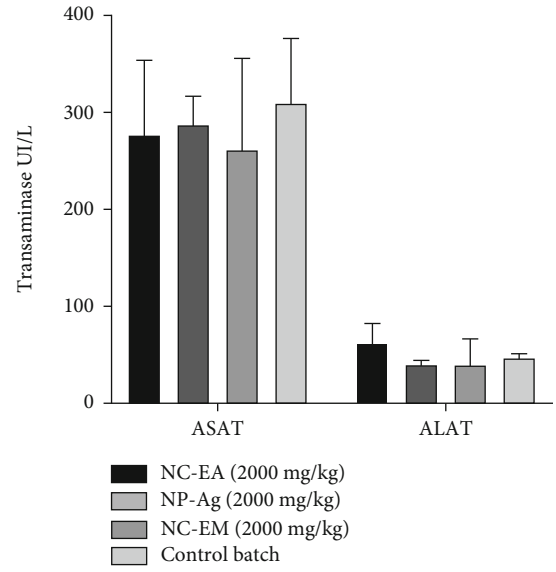


Figure 12: ALAT and ASAT levels in rats subjected to the acute toxicity test for different samples and the control.

showed spherical and aggregate nanograins (Figures 6 and 7). Aggregates have been obtained by several researchers for green-synthesized metallic nanoparticles [27, 30]. The SEM images of NCs depicted ovoid capsule clusters. Other forms such as spherical nanocapsules were obtained by Servat-Medina et al. [16]. The formation of ovoid clusters is probably related to the unique chitosan/tripolyphosphate ratio that was used. In 2019, Pratiwi et al. demonstrated that the chitosan/tripolyphosphate ratio influences the size and shape of particles [17]. Energy dispersive X-ray (EDX) spectroscopy provides elemental mapping of AgNPs and NCs. Carbon, oxygen, and sulfur were present in the NC spectrum. They are the main elements that constitute organic matter and are therefore found in most classes of metabolites identified in the plant extracts and the chitosan used in this study. In addition to these elements, silver, chlorine, and aluminum were found in AgNPs, indicating that synthesized silver nanomaterial transports organics at its interface (Table 4). Similar results were reported by Slepička et al. in 2020 on silver nanoparticles mediated by *Selaginella myosurus* [27] and Choudhary et al. in 2019 on chitosan nanocapsules [31].

3.7. Antimicrobial Activities. The antimicrobial activities of synthesized nanoderivatives (AgNPs, NC-AE, and NC-ME), extracts (AE, ME, and NC-E), and reference drugs (ketoconazole and ciprofloxacin) were determined (Tables 5–7). Although empty capsules produced no effect, NCs exhibited superior MIC compared to the corresponding extracts. AgNPs showed significant bactericidal activity against *Candida spp* with an MBC/MIC ratio of 2.000. Ciprofloxacin showed significant activity against *Escherichia coli* and *Salmonella typhi* with MBC/MIC ratios of 1.000 and

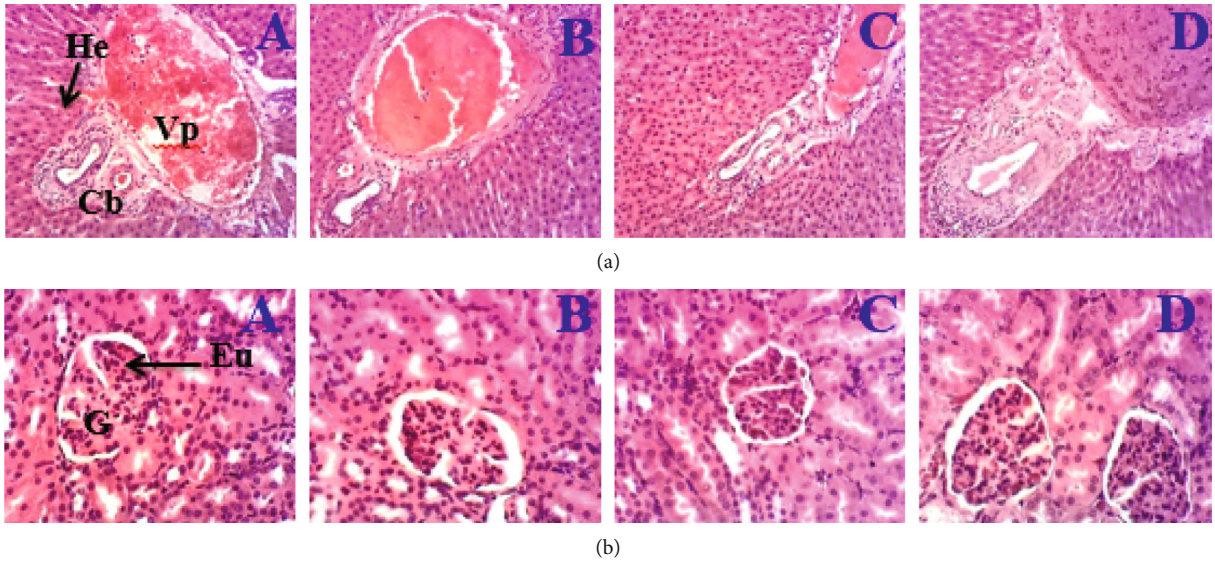


Figure 13: (a) Liver and (b) kidney microphotographs (×100 and ×200, respectively) of treated rats during the acute toxicity test. A: control; B: NC-AE; C: AgNPs; D: NC-ME; Vp: portal vein; He: hepatocyte; Cb: bile canaliculus; G: glomerulus; Eu: urinary space.

2.000, respectively. Ketoconazole induced an MIC of 2.10^{-6} mg/mL against *Candida* spp. Considering that chitosan acts as a transport vehicle for secondary metabolites, Ilk et al. in 2017 demonstrated that chitosan nanocapsules, due to their nanometric size, can easily penetrate bacterial walls and release their contents directly at the active site. This increases the concentration of active substances at the site of action, thereby leading to increased antimicrobial activity [32].

AgNPs have been shown to have efficacy comparable to that of ciprofloxacin against *Salmonella spp* but less efficacy against *Escherichia coli*. These activities are linked on one hand to the possibility of silver nanoparticles penetrating the microbial cell and acting on various sites. On the other hand, the synthesized AgNPs are coated with molecules from the aqueous extract that could also have intrinsic antimicrobial properties [33]. Thus, AgNPs could play a beneficial role as a vehicle allowing for the delivery of Ag^+ ions and/or molecules from the extract to their site of action in a synergetic situation.

The high activity of AgNPs compared to nanocapsules can be explained by the sizes of the different structures. The nanocapsules synthesized by the ionic gelation method are generally a few hundred nanometers in size, while AgNPs are much smaller (13.5 nm) [16, 17]. This difference in the size of AgNPs compared to nanocapsules favors the delivery of AgNPs. In addition to size and surface chemistry or functionalization, factors including size distribution, morphology, surface charge, capping agents, hydrophobicity, and porosity may influence the biological activity of inorganic nanoparticles [34, 35].

3.8. Oral Acute Toxicity Profile. In this study, the oral administration of synthesized nanoderivatives in Wistar rats suggests the probable absence of toxicity of NC-ME. No change in behavior or body weight was observed in any of the tested rats as compared to the control group during the experimental period (Figure 8). Nonetheless, a significant increase ($p < 0.05$) in lung mass and a significant decrease ($p < 0.01$) in creatinemia were observed in NC-EA-treated rats as compared to the control (Figures 9 and 10). AgNPs significantly ($p < 0.05$) increased uremia (Figure 11) and significantly ($p < 0.05$) decreased creatinemia as compared to the control. However, the differences remained within the range of normal values [36]. These observed effects can be attributed to strychnine and related compounds, as found in other species of the genus Strychnos by Disengomokaa in 1983 [11]. In fact, strychnine, probably present within the *Strychnos phaeotricha* liana bark aqueous extract, has been reported to induce pulmonary edema [37]. The differences observed in creatinine and uremia remain within the range of normal values proposed by Etienne in 2005 [38]. Concerning alanine aminotransferase (ASAT) and aspartate aminotransferase (ALAT), no statistical difference was found between treated rats and the control (Figure 12). In addition, histological analyses of the kidneys and liver of the treated rats revealed no abnormalities as compared to the control (Figure 13). The lethal dose 50 (LD_{50}) was estimated to be greater than 2000 mg/kg following the recommendation of the OECD since no deaths were noted [20]. Moreover, the studies reviewed implied disadvantages of biologically synthesized metallic nanoparticles. For example, nanoparticles' genotoxicity varies case-by-case and is highly dependent on parameters like synthesis, the biological source, or the applied assay [39]. Other studies have revealed that in addition to the directly reactive oxygen species production and antioxidant defense inhibition induced by AgNPs, the upregulation of prooxidant genes is involved in the oxidative injury caused by these NPs [40]. The authors of these studies must translate the research results to the global market.

4. Conclusion

The synthesis and characterization of silver nanoparticles and chitosan nanocapsules with *Strychnos phaeotricha* liana bark extracts and the evaluation of their antimicrobial activity and oral acute toxicity on Wistar rats were presented. The characterization analyses made it possible to define the diameter of the silver nanoparticles at 13.5 nm; meanwhile, the encapsulation rates were found to be 73.5% and 69.3% for aqueous and methanolic extracts, respectively. Metabolites were confirmed at the interface of silver nanoparticles and encapsulated in chitosan. Pulverized liana bark extracts were found to be capable of generating silver nanoparticles and chitosan nanocapsules with potent antimicrobial activity. These nanoderivatives did not show any harmful signs in relation to the acute oral toxicity tests carried out. Silver nanoparticles proved to be more effective than chitosan nanocapsules in inhibiting and/or destroying the microorganisms. This work suggests a new antimicrobial therapeutic axis that entails transporting metabolites to the surface or encapsulated in chitosan to fight microbial resistance while preserving biodiversity and the environment.

Data Availability

Data are available on request.

Conflicts of Interest

The authors declare no conflicts of interest.

Acknowledgments

The authors thank the Multidisciplinary Laboratory of the Faculty of Medicine and Pharmaceutical Sciences, Department of Pharmaceutical Sciences for technical support. Support of Word University Service under APA 2668 for providing part equipment used is appreciated. FEM thanks the German Academic Exchange Service DAAD for a generous Professor Fellowship (grant No. 768048). PBEK thanks the FIS for the support grant No. I-1-F-6137-1.

References

[1] J. Estelrich, M. Quesada-Pérez, J. Forcada, and J. Callejas-Fernández, "chapter 1:Introductory Aspects of Soft Nanoparticles," in *Soft Nanoparticles for Biomedical Applications*, pp. 1–18, The Royal Society of Chemistry, 2014.

[2] D. Sharma, S. Kanchi, and K. Bisetty, "Biogenic synthesis of nanoparticles: a review," *Arabian Journal of Chemistry*, vol. 12, pp. 3576–3600, 2015.

[3] A. Domard, M. Rinaudo, and C. Terrassin, "New method for the quaternization of chitosan," *International Journal of Biological Macromolecules*, vol. 8, no. 2, pp. 105–107, 1986.

[4] J. C. Leroux, E. Allemann, E. Doelker, and R. Gurny, "New approach for the preparation of nanoparticles by an emulsification-diffusion method," *European Journal of Pharmaceutics and Biopharmaceutics*, vol. 41, pp. 14–14, 1995.

[5] H. Fessi, F. Puisieux, J. P. Devissaguet, N. Ammoury, and S. Benita, "Nanocapsule formation by interfacial polymer deposition following solvent displacement," *International Journal of Pharmaceutics*, vol. 55, no. 1, pp. R1–R4, 1989.

[6] J. P. Rao and K. E. Geckeler, "Polymer nanoparticles: preparation techniques and size-control parameters," *Progress in Polymer Science*, vol. 36, no. 7, pp. 887–913, 2011.

[7] H. Hosseinzadeh, F. Atyabi, R. Dinarvand, and S. N. Ostad, "Chitosan-Pluronic nanoparticles as oral delivery of anticancer gemcitabine: preparation and in vitro study," *International Journal of Nanomedicine*, vol. 7, pp. 1851–1863, 2012.

[8] R. Bodmeier, K. H. Oh, and Y. Pramar, "Preparation and evaluation of drug-containing chitosan beads," *Drug Development and Industrial Pharmacy*, vol. 15, no. 9, pp. 1475–1494, 1989.

[9] A. J. M. Leeuwenberg, *Flore du Cameroun : Loganiacées*, Muséum national d'histoire naturelle, Paris 5e, 1972.

[10] L. Bohlin, F. Sandberg, and W. Rolfsen, "Screening of African Strychnos species for convulsant and muscle relaxant effects," *Acta Pharmaceutica Suecica*, vol. 14, p. 62, 1977.

[11] I. Disengomokaa, "Medicinal plants in Zaire. Part II used for child's respiratory diseases," *Journal of Ethnopharmacology*, vol. 8, no. 3, pp. 265–277, 1983.

[12] A. Bouquet and A. Fouret, "Recherches chimiques préliminaires sur les plantes médicinales du Congo Brazzaville," *Fitoterapia*, vol. 46, no. 4, pp. 175–191, 1975.

[13] F. Eya'ane Meva, M. L. Segnou, C. Okalla Ebongue et al., "Spectroscopic synthetic optimizations monitoring of silver nanoparticles formation from Megaphrynium macrostachyum leaf extract," *Brazilian Journal of Pharmacognosy*, vol. 26, no. 5, pp. 640–646, 2016.

[14] E. Nnanga Nga, L. Soppo, A. Nokam et al., "Identification des familles de composés bioactifs et métabolites secondaires de *Trichoscypha odonii* de Wild justifiant son usage en médecine traditionnelle," *Health Sciences and Disease*, vol. 20, no. 6, 2019.

[15] F. Eya'ane Meva, M. L. Segnou, C. Okala Ebongue et al., "Unexplored vegetal green synthesis of silver nanoparticles : a preliminary study with *Corchorus olitorus* Linn and *Ipomea batatas* (L) Lam," *African Journal of Biotechnology*, vol. 15, no. 10, pp. 341–349, 2016.

[16] L. Servat-Medina, A. González-Gómez, F. Reyes-Ortega et al., "Chitosan–tripolyphosphate nanoparticles as Arrabidaea chica standardized extract carrier: synthesis, characterization, biocompatibility, and antiulcerogenic activity," *International Journal of Nanomedicine*, vol. 10, pp. 3897–3909, 2015.

[17] G. Pratiwi, R. Martien, and R. Murwanti, "Chitosan nanoparticle as a delivery system for polyphenols from meniran extract (*Phyllanthus niruri* l.): formulation, optimization, and immunomodulatory activity," *International Journal of Pharmaceutics*, vol. 11, no. 2, pp. 50–58, 2019.

[18] J. B. Harborne, J. B. Harborne, and J. B. Harborne, "Recent advances in chemical ecology," *Natural Product Reports*, vol. 16, no. 4, pp. 509–523, 1999.

[19] S. M. Evans, "Anti-fouling materials," in *Encyclopedia of Ocean Sciences*, pp. 170–176, Elsevier, 2001.

[20] Organisation for Economic Co-operation and Development, *Guidelines for the Testing of Chemicals*, 2008, Section 4. https://www.oecd-ilibrary.org/environment/oecd-guidelines-for-the-testing-of-chemicals-section-4-health-effects_20745788.

[21] Société francaise de Microbilogie, *Determination de la sensibilité aux antibiotiques*, CASFM/EUCAST, France, 2019.

[22] E. Matuschek, D. J. F. Brown, and G. Kahlmeter, "Development of the EUCAST disk diffusion antimicrobial susceptibility testing method and its implementation in routine microbiology laboratories," *Clinical Microbiology and Infection*, vol. 20, no. 4, pp. 0255–0266, 2014.

[23] A. Launay, *Pharmacognosie, phytochimie, plantes médicinales*, J. Bruneton, Ed., vol. 15no. 1, 2016Éditions Lavoisier Tec & Doc, 5th edition, 2016.

[24] M. Zou, M. Du, H. Zhu, C. Xu, N. Li, and Y. Fu, "Synthesis of silver nanoparticles in electrospun polyacrylonitrile nanofibers using tea polyphenols as the reductant," *Polymer Engineering & Science*, vol. 53, no. 5, pp. 1099–1108, 2013.

[25] A. M. Awwad, N. M. Salem, and A. O. Abdeen, "Green synthesis of silver nanoparticles using carob leaf extract and its antibacterial activity," *International Journal of Industrial Chemistry*, vol. 4, no. 1, pp. 1–6, 2013.

[26] S. H. Lee and B. H. Jun, "Silver nanoparticles: synthesis and application for nanomedicine," *International Journal of Molecular Sciences*, vol. 20, no. 4, p. 865, 2019.

[27] P. Slepička, N. S. Kasálková, J. Siegel, Z. Kolská, and V. Švorčík, "Methods of gold and silver nanoparticles preparation," *Materials*, vol. 13, no. 1, pp. 1–22, 2020.

[28] P. B. Ebanda Kedi, F. Eya'ane Meva, L. Kotsedi et al., "Eco-friendly synthesis, characterization , in vitro and in vivo anti-inflammatory activity of silver nanoparticle-mediated *Selaginella myosurus* aqueous extract," *International Journal of Nanomedicine*, vol. 13, pp. 8537–8548, 2018.

[29] S. Sreekumar, F. M. Goycoolea, B. M. Moerschbacher, and G. R. Rivera-rodriguez, "Parameters influencing the size of chitosan-TPP nano- and microparticles," *Scientific Reports*, vol. 8, no. 1, pp. 1–11, 2018.

[30] K. A. Selvam, M. Suriyakumar, J. Devanathan et al., "Synthesis of Ag-NPs from extracts of Persea americana and its antimicrobial effects in human pathogens," *NanoNEXT*, vol. 1, no. 8, pp. 10–18, 2020.

[31] R. C. Choudhary, S. Kumari, R. V. Kumaraswamy et al., *Characterization Methods for Chitosan-Based Nanomaterials*, R. Prasad, Ed., Plant Nanobionics, Nanotechnology in the Life Sciences, Switzerland, 2019, Chapter 5.

[32] S. Ilk, N. Saglam, and M. Özgen, "Kaempferol loaded lecithin/chitosan nanoparticles: preparation, characterization, and their potential applications as a sustainable antifungal agent," *Artificial Cells, Nanomedicine and Biotechnology*, vol. 45, no. 5, pp. 907–916, 2017.

[33] R. Y. Pelgrift and A. J. Friedman, "Nanotechnology as a therapeutic tool to combat microbial resistance," *Advanced Drug Delivery Reviews*, vol. 65, no. 13-14, pp. 1803–1815, 2013.

[34] H. Barabadi, H. Vahidi, K. D. Kamali, M. Rashedi, and M. Saravanan, "Antineoplastic biogenic silver nanomaterials to combat cervical cancer: a novel approach in cancer therapeutics," *Journal of Cluster Science*, vol. 31, no. 4, pp. 659–672, 2020.

[35] M. Saravanan, H. Barabadi, B. Ramachandran, G. Venkatraman, and K. Ponmurugan, "Chapter Eleven - Emerging plant-based anti-cancer green nanomaterials in present scenario," in *Comprehensive Analytical Chemistry*, S. K. Verma and A. K. Das, Eds., vol. 87, pp. 291–318, Elsevier, 2019.

[36] C. R. Laboratories, *Baseline Hematology and Clinical Chemistry Values for Charles River Wistar Rats-(CRL: (WI) BR) as Function Sex and Age*, Technical Bulletin, 1982.

[37] A. Lages, J. Pinho, R. Alves, and C. Capela, "Strychnine intoxication : a case report," *Elmer Press*, vol. 4, no. 6, pp. 385–388, 2013.

[38] A. d. L. Etienne, "Dominantes pathologiques chez le rat domestique," *vet prat de France*, vol. 89, no. 1, pp. 60–76, 2005.

[39] H. Barabadi, M. Najafi, H. Samadian et al., "A systematic review of the genotoxicity and antigenotoxicity of biologically synthesized metallic nanomaterials: are green nanoparticles safe enough for clinical marketing?," *Medicina*, vol. 55, no. 8, 2019.

[40] K. Mortezaee, M. Najafi, H. Samadian, H. Barabadid, A. Azarnezhade, and A. Ahmadif, "Redox interactions and genotoxicity of metal-based nanoparticles: a comprehensive review," *Chemico-Biological Interactions*, vol. 312, article 108814, 2019.